Harmonic Droop Controller to Reduce the Voltage Harmonics of Inverters

Qing-Chang Zhong, *Senior Member, IEEE*

***Abstract*—In this paper, the load and/or grid connected to an inverter is modelled as the combination of voltage sources and current sources at harmonic frequencies. As a result, the system can be analysed at each individual frequency, which avoids the difficulty in defining the reactive power for a system with different frequencies because it is now defined at each individual frequency. Moreover, a droop control strategy is developed for systems delivering power to a constant current source, instead of a constant voltage source. This is then applied to develop a harmonic droop controller so that the right amount of harmonic voltage is added to the inverter reference voltage to compensate the harmonic voltage dropped on the output impedance due to the harmonic current. This forces the output voltage at the individual harmonic frequency close to zero and improves the THD of the output voltage considerably. Both simulation and experimental results are provided to demonstrate that the proposed strategy can significantly improve the voltage THD.**

Keywords: Power quality, total harmonic distortion (THD), droop control, parallel operation of inverters, proportional load sharing, harmonic droop controller

I. Introduction

Nowadays, more and more distributed generation and renewable energy sources, e.g. wind, solar and tidal power, are developed. They often form microgrids via power inverters [1]–[5], which may or may not be connected to the grid. One of the major problems in these applications is the harmonics in the voltage provided by the inverters. There are two sources of harmonics: one is from the inverters (e.g. because of the pulse-width-modulation and the switching) and the other is from loads or the grid. The majority of loads today are nonlinear and generate harmonic currents when a purely sinusoidal voltage supply is provided. These harmonic currents then cause harmonic components in the voltage because of the impedances in the distribution network and, also, inside the voltage source. Of course, harmonic voltages then cause harmonic currents as well. The odd multiples of the 3rd harmonic (3rd, 9th, 15th, 21st ...), i.e. the $6n-3$ harmonics, are called triplen harmonics. These currents on a 3-phase system are zero-sequence harmonics, which are additive in the neutral line and cause particular concern. The $6n-1$ harmonics are negative-sequence harmonics and can cause problems to electrical machines because these harmonics create a negative torque and attempt to drive the machines in reverse. Harmonics are not desirable because they cause overheating, increased losses, decreased kVA capacity, neutral line overloading, distorted voltage and current waveforms etc. It has become a very serious issue in modern power systems. Hence, stringent regulations have been put into place [6], [7]. The total harmonic distortion (THD) of voltages and currents needs to be maintained low, often below 5%. This paper focuses on the cancellation of harmonics in voltage. For the cancellation of current harmonics, active power filters can be adopted. See, for example, [8]–[10].

Several feedback control schemes have been proposed to reduce the voltage THD of inverters. Deadbeat or hysteresis controllers [11] are some examples. Repetitive control theory [12], which is regarded as a simple learning control method, provides an alternative to eliminate periodic errors in dynamic systems, using the internal model principle [13]. Such a closed-loop system can deal with a very large number of harmonics simultaneously, as it has high gains at the fundamental and all harmonic frequencies of interest. It has been successfully applied to constant-voltage constant-frequency (CVCF) PWM inverters [14]–[19], grid-connected inverters [2], [6], [20] and active filters [21], [22] to obtain very low THD. Strategies have been developed to maintain low THD in the current exchanged with the grid [6], in the microgrid voltage [20], [23] and in both the current exchanged with the grid and the microgrid voltage at the same time [24]. A cooperative harmonic filtering strategy was proposed in [25] to share the harmonic var [26] among distributed inverters, which has the capability of improving the voltage THD. The drawback is that extensive experiments are needed to determine the reference value for the harmonic var.

It is well understood [27] that the output impedance of an inverter plays an important role in power sharing and a droop controller for inverters with resistive output impedances was proposed for sharing linear and nonlinear loads [28]. The output impedance of an inverter also plays a critical role in reducing the THD of the output voltage [29]. The voltage THD could be improved via reducing the output impedance. In this paper, another approach is proposed to reduce the voltage THD. Its development involves three steps. Firstly, the load or grid connected to an inverter is modelled as the combination of voltage sources and current sources at harmonic frequencies. Based on this, the voltage harmonics can be treated individually at each harmonic frequency. If the right amount of harmonic voltage is added to the reference

Manuscript received December 10, 2010. Accepted for publication April 4, 2011.

A preliminary version of this paper was presented at the 18th IFAC World Congress held in Milano, Italy in September 2011.

The author is with the Department of Aeronautical and Automotive Engineering, Loughborough University, Leicestershire LE11 3TU, United Kingdom. Tel: +44-1509-227 223, fax: +44-1509-227 275, Email: zhongqc@ieee.org.

voltage for the inverter, then the harmonic component in the output voltage can be made zero. Secondly, a droop control strategy is developed to deliver power to a constant current source/sink[1]. Finally, a harmonic droop control strategy is proposed to reduce individual harmonics. Effectively, it means that the power sharing or droop control should be done at each individual harmonic frequency, which avoids the difficulty in defining/calculating reactive power at different frequencies together [26], [30]. Simulation and experimental results are provided to show that the proposed strategy could considerably improve voltage THD.

The rest of the paper is organised as follows. In Section II, a method to model inverter systems is proposed. In Section III, after reviewing how the power is delivered to a constant voltage source through an impedance, how the power is delivered to a constant current source through an impedance is developed. This is then applied to develop a harmonic droop control strategy in Section IV to reduce voltage harmonics. Simulation results and experimental results are given in Sections V and VI, respectively, followed by conclusions made in Section VII.

II. Model of an Inverter System

It is widely known that a (linear) circuit having supplies/sinks with different frequencies can be analysed separately at each frequency according to the superposition theorem. Here, this will be applied to inverter systems.

For an inverter, whether it is connected to a load, a grid or both, the mathematical model of the system can be illustrated as shown in Figure 1(a), where the inverter is modelled as a voltage reference v_r with an output impedance $Z_o(s)$ and the load is modelled as the combination of voltage sources and current sources. The terminal or output voltage is

$$v_o = v_{o1} + \Sigma_{h=2}^{\infty} v_{oh}$$

with $v_{o1} = \sqrt{2}V_{o1}\sin(\omega^* t)$ and $v_{oh} = \sqrt{2}V_{oh}\sin(h\omega^* t + \psi_h)$, where ω^* is the rated fundamental angular frequency of the system, V_{o1} is the RMS voltage of the fundamental component and V_{oh} is the RMS voltage of the h-th harmonic component. The output or load current is described as

$$i = \Sigma_{h=1}^{\infty} i_h,$$

with $i_h = \sqrt{2}I_h \sin(h\omega^* t + \phi_h)$. This represents the effect of nonlinear loads or harmonic currents and forces the current flowing through the series of voltage sources to be zero. The voltage reference v_r in the general case is described as

$$v_r = v_{r1} + \Sigma_{h=2}^{\infty} v_{rh}$$

with $v_{r1} = \sqrt{2}E\sin(\omega^* t + \delta)$ and $v_{rh} = \sqrt{2}E_h \sin(h\omega^* t + \delta_h)$. In many cases, in particular, when a droop controller is used in the inverter, E_h is often set to be zero. In this paper, E_h will be designed to be non-zero to make v_{oh} close to zero.

This circuit can be analysed after decomposing it into multiple circuits at each harmonic frequency, according to the superposition theorem. The h-th harmonic circuit of the system is shown in Figure 1(b). The load of the circuit $\frac{V_{o1}}{I_1}\angle - \phi_1$ at the fundamental frequency[2] is expressed as the combination of the voltage source $V_{o1}\angle 0^\circ$ and the current source $I_1\angle\phi_1$. If v_{oh} ($h \neq 1$) is close to zero, then what is left in the right hand side of Figure 1(b) is a current source i_h.

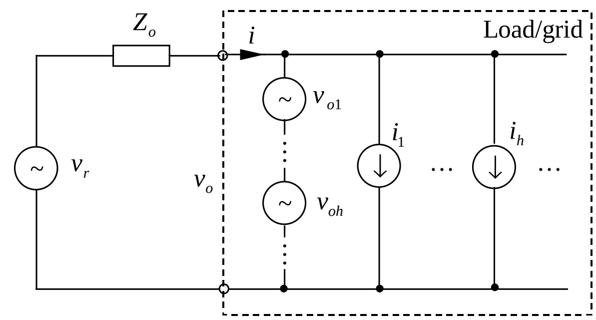

(a) One circuit including all harmonics

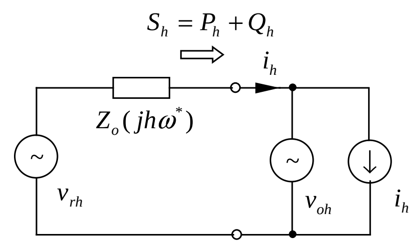

(b) The circuit at the h-th harmonic frequency

Figure 1. The model of an inverter connected to a load/grid

The main function of an inverter (or a generator) is to supply the load with the real power and reactive power at the right voltage level and at the right frequency, which are regulated by industrial standards and/or law. To be more precise, this should be done *at the fundamental frequency*, without harmonics. When multiple inverters are connected in parallel, they should also share the real power and reactive power in proportion to their capacity, again *at the fundamental frequency*. Then, what happens with harmonics? Ideally, the harmonics in the output voltage are expected to be 0, i.e., $v_{oh} = 0$ ($h = 2, 3, \cdots$), even when there are harmonics in the current i. This can be achieved when the voltage drop of the h-th harmonic current $\sqrt{2}I_h \sin(h\omega^* t + \phi_h)$ on the output impedance $Z_o(j\omega)$ is the same as the h-th harmonic component of the voltage reference $\sqrt{2}E_h \sin(h\omega^* t + \delta_h)$, i.e., when

$$E_h = I_h\left|Z_o(jh\omega^*)\right| \quad \text{and} \quad \delta_h = \phi_h + \angle Z_o(jh\omega^*). \tag{1}$$

In this paper, this idea will be exploited to design a controller for the inverter so that the harmonics in the output voltage are considerably reduced, after filling a gap in the theory of power delivery through an impedance.

III. Power Delivered through an Impedance

It has been well understood how real power and reactive power are delivered through an impedance, whether it is in-

[1] In this paper, a source is used to represent a source or a sink.

[2] Note that the phasors in this paper may be at different frequencies, which should be clear from the context.

ductive, resistive, capacitive or other types, when the terminal voltage is more or less maintained constant as a voltage source. Moreover, power sharing schemes, e.g., different droop control strategies [27]–[29], [31]–[34], have been developed for this case. However, it has not been studied how real power and reactive power are delivered when the terminal is connected to a current source with a constant current. In this section, this is developed after reviewing how the power is delivered to a constant voltage source.

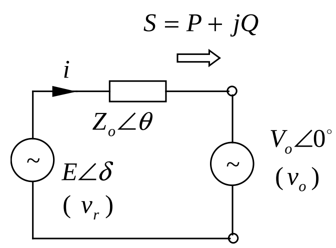

(a) To a voltage source

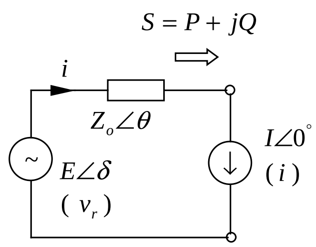

(b) To a current source

Figure 2. Real power and reactive power delivered by a voltage source through an impedance

A. Power delivered to a voltage source

Figure 2(a) illustrates a voltage source v_r delivering power to another voltage source $V_o\angle 0^\circ$ through an impedance $Z_o\angle\theta$. The current flowing through the terminal is

$$\begin{aligned}\bar{I} &= \frac{E\angle\delta - V_o\angle 0^\circ}{Z_o\angle\theta} \\ &= \frac{E\cos\delta - V_o + jE\sin\delta}{Z_o\angle\theta}.\end{aligned}$$

The real power and reactive power delivered to the terminal via the impedance are then obtained as

$$\begin{aligned}P &= (\frac{EV_o}{Z_o}\cos\delta - \frac{V_o^2}{Z_o})\cos\theta + \frac{EV_o}{Z_o}\sin\delta\sin\theta, \\ Q &= (\frac{EV_o}{Z_o}\cos\delta - \frac{V_o^2}{Z_o})\sin\theta - \frac{EV_o}{Z_o}\sin\delta\cos\theta,\end{aligned}$$

where δ is the phase difference between the supply and the terminal, often called the power angle.

For an inductive impedance, $\theta = 90^\circ$. Then

$$P = \frac{EV_o}{Z_o}\sin\delta \quad \text{and} \quad Q = \frac{EV_o}{Z_o}\cos\delta - \frac{V_o^2}{Z_o}.$$

When δ is small,

$$P \approx \frac{EV_o}{Z_o}\delta \quad \text{and} \quad Q \approx \frac{V_o}{Z_o}E - \frac{V_o^2}{Z_o},$$

and, roughly,

$$P \sim \delta \quad \text{and} \quad Q \sim E,$$

where $\sim$ means in proportion to. As a result, the conventional droop control strategy for an inductive Z_o takes the form

$$\begin{aligned}E_i &= E^* - n_i Q_i, \\ \omega_i &= \omega^* - m_i P_i,\end{aligned}$$

where E^* is the rated RMS voltage of the inverter. This strategy is sketched in Figure 3(a).

For a resistive impedance, $\theta = 0^\circ$. Then

$$P = \frac{EV_o}{Z_o}\cos\delta - \frac{V_o^2}{Z_o} \quad \text{and} \quad Q = -\frac{EV_o}{Z_o}\sin\delta.$$

When δ is small,

$$P \approx \frac{V_o}{Z_o}E - \frac{V_o^2}{Z_o} \quad \text{and} \quad Q \approx -\frac{EV_o}{Z_o}\delta,$$

and, roughly,

$$P \sim E \quad \text{and} \quad Q \sim -\delta.$$

Hence, the conventional droop control strategy takes the form

$$\begin{aligned}E_i &= E^* - n_i P_i, \\ \omega_i &= \omega^* + m_i Q_i,\end{aligned}$$

This is sketched in Figure 3(b).

If the impedance is capacitive, then $\theta = -90^\circ$ and

$$P = -\frac{EV_o}{Z_o}\sin\delta \quad \text{and} \quad Q = -\frac{EV_o}{Z_o}\cos\delta + \frac{V_o^2}{Z_o}.$$

When δ is small,

$$P \approx -\frac{EV_o}{Z_o}\delta \quad \text{and} \quad Q \approx -\frac{V_o}{Z_o}E + \frac{V_o^2}{Z_o},$$

and, roughly,

$$P \sim -\delta \quad \text{and} \quad Q \sim -E.$$

Hence, the strategy following the conventional droop control strategy for inverters with capacitive output impedances takes the form

$$\begin{aligned}E_i &= E^* + n_i Q_i, \\ \omega_i &= \omega^* + m_i P_i,\end{aligned}$$

This is sketched in Figure 3(c).

B. Power delivered to a current source

Figure 2(b) illustrates a voltage source v_r delivering power to a current source $I\angle 0^\circ$ through an impedance $Z_o\angle\theta$. Then, the terminal voltage is

$$\begin{aligned}\bar{V}_o &= E\angle\delta - Z_o I\angle\theta \\ &= E\cos\delta - Z_o I\cos\theta + j(E\sin\delta - Z_o I\sin\theta)\end{aligned}$$

and the real power and reactive power delivered to the terminal are, respectively,

$$P = EI\cos\delta - Z_o I^2\cos\theta, \tag{2}$$
$$Q = EI\sin\delta - Z_o I^2\sin\theta. \tag{3}$$

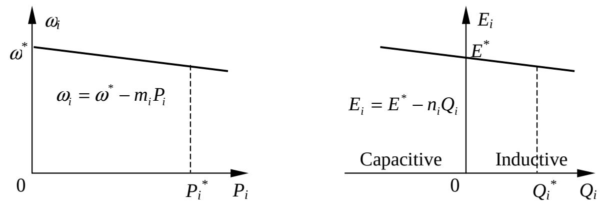

(a) for an inductive Z_o

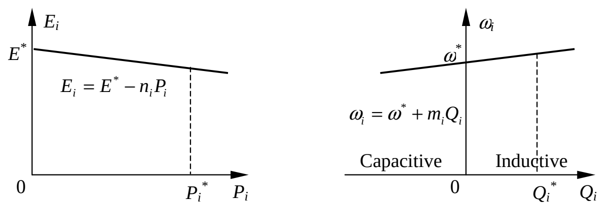

(b) for a resistive Z_o

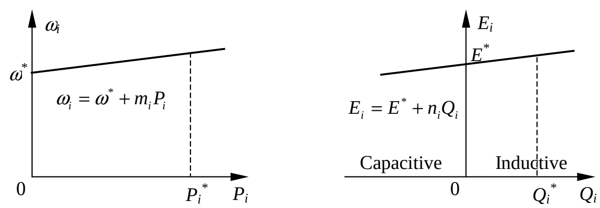

(c) for a capacitive Z_o

Figure 3. Droop control for inverters maintaining a constant output voltage

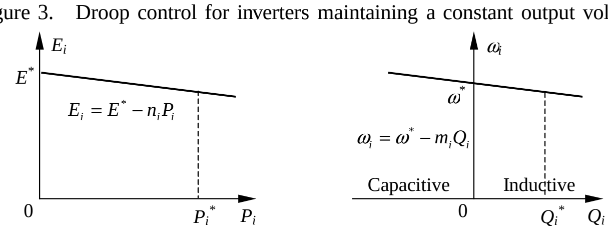

Figure 4. Droop control for inverters maintaining a constant output current (for any type of impedances)

Again, δ is the phase difference between the supply (voltage) and the terminal (current). When δ is small,

$$P \approx EI - Z_o I^2 \cos\theta,$$
$$Q \approx EI\delta - Z_o I^2 \sin\theta.$$

Hence, roughly,

$$P \sim E \quad \text{and} \quad Q \sim \delta$$

for any type of impedance $Z_o\angle\theta$. This is quite different from the case with a voltage source, where these relationships change with the type of the impedance. The conventional droop control strategy should then take the form

$$E_i = E^* - n_i P_i, \tag{4}$$
$$\omega_i = \omega^* - m_i Q_i. \tag{5}$$

This strategy, as sketched in Figure 4, is different from any of the droop control strategies when the power is delivered to a voltage source. Note that, in order to make sure that the $P-E$ loop and the $Q-\omega$ loop are of a negative feedback, respectively, so that the droop controller is able to regulate the frequency and the voltage, the signs before $n_i P_i$ and $m_i Q_i$ are all negative, which makes them droop terms. The main advantage of this scheme is that it does not depend on the type of the impedance and, hence, it can be used for any type of impedances. This facilitates the controller design, without the need of checking the impedance type at the corresponding harmonics. The purpose of this paper is to develop a strategy to improve the voltage THD based on this, instead of developing a control strategy for parallel operation of power sources. This is being investigated and will be reported separately.

Note that $P = 0$ and $Q = 0$ when

$$E = Z_o I \qquad \text{and} \qquad \delta = \theta,$$

according to (2) and (3). This is another way to express (1) and can be used to reduce or even eliminate harmonics in the output voltage.

IV. Reduction of Harmonics in the Output Voltage

In this section, a strategy will be proposed to reduce voltage harmonics via injecting harmonics into the voltage reference.

As discussed above, in order to force the h-th harmonics in the output voltage of an inverter to be (nearly) zero, the voltage source v_{oh} in Figure 1(b) needs to be zero. In other words, the real power and reactive power delivered to the current source i_h in Figure 1(b) should be 0. As a result, the voltage set-point E^* for the droop controller obtained in (4) should be 0 for the h-th harmonics ($h \neq 1$). The frequency set-point should simply be set as the h-th harmonic frequency. This leads to the following h-th harmonic droop controller:

$$E_h = -n_h P_h, \tag{6}$$
$$\omega_h = h\omega^* - m_h Q_h, \tag{7}$$

where P_h and Q_h are the real power and reactive power at the terminal for the h-th harmonic frequency, and n_h and m_h are the corresponding droop coefficients. Here, the subscripts of the relevant variables are changed to reflect the h-th harmonics. The reference voltage v_{rh} at the h-th harmonic frequency can then be formed with the RMS value E_h and the phase angle generated from the integration of ω_h. In practice, instead of generating a harmonic frequency ω_h from (7), it can be obtained from $h\omega t$ with the addition of δ_h, which is integrated from $-m_h Q_h$. Here, ωt is the phase of the voltage reference at the fundamental frequency. This leads to the proposed h-th harmonic droop controller shown in Figure 5. As explained above, it does not depend on the type of the output impedance at the h-th harmonic frequency, which could be resistive, inductive, capacitive or even complex.

Since the controller (6) in the voltage channel is a proportional controller, there will be a static error and V_{oh} will not be exactly zero (but close to zero). The V_{oh} can be calculated approximately via

$$V_{oh} \approx E_h - |Z_o(jh\omega^*)|\, I_h \approx -n_h V_{oh} I_h - |Z_o(jh\omega^*)|\, I_h.$$

That is,

$$V_{oh} \approx -\frac{|Z_o(jh\omega^*)|\, I_h}{n_h I_h + 1}.$$

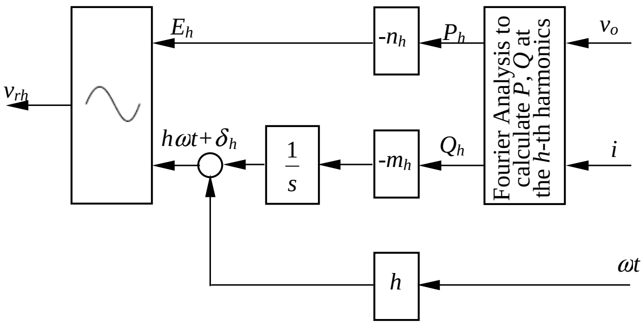

Figure 5. The proposed h-th harmonic droop controller ($h \neq 1$)

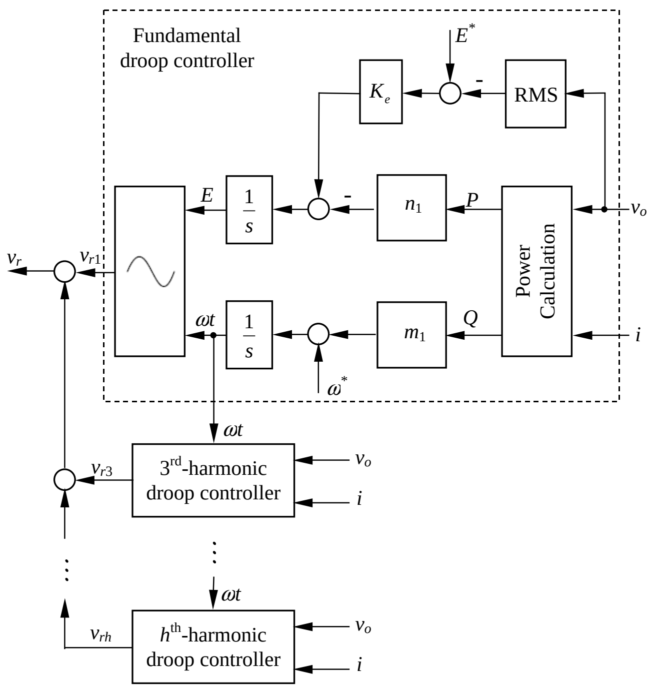

Figure 6. The proposed droop controller consisting of a robust droop controller at the fundamental frequency and several harmonic droop controllers at individual harmonic frequencies

Its contribution to the voltage THD is approximately $\frac{|Z_o(jh\omega^*)|I_h}{(n_h I_h+1)E^*}$. The smaller the output impedance at the harmonic frequency $h\omega^*$, the smaller the THD. Hence, strategies like the one proposed in [29] can be adopted to reduce $|Z_o(jh\omega^*)|$ and the voltage THD. The parameter n_h can be chosen big to make V_{oh} small as long as the system remains stable. As a rule of thumb, the tuning can be started with

$$n_h = \frac{|Z_o(jh\omega^*)|}{\gamma E^*},$$

with which the contribution of the h-harmonic component to the THD is about γ. If this causes instability, then it can be reduced. The parameter m_h can be determined in the same way as m_1 because $\frac{m_h Q_h^*}{h\omega^*}$ is the frequency drop ratio at the h-th harmonics, which should be the same as that at the fundamental frequency, i.e., $\frac{m_1 Q^*}{\omega^*}$. Hence,

$$m_h = m_1 \frac{hQ^*}{Q_h^*}.$$

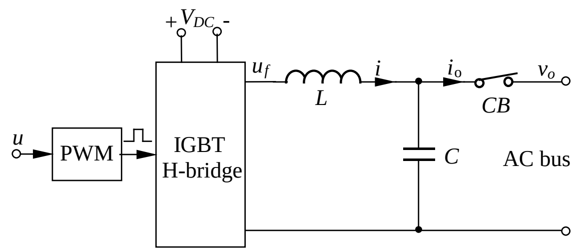

(a) A descriptive circuit

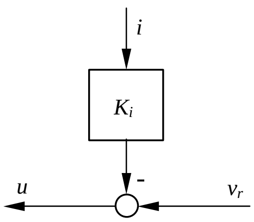

(b) An inner-loop current controller

Figure 7. Controller design to achieve a resistive output impedance

As a result, m_h is often much larger than m_1 because Q_h^* is often much smaller than hQ^*.

In order to reduce multiple harmonics in the output voltage, several harmonic droop controllers corresponding to the harmonic orders can be included in the controller to generate the required $\Sigma_h v_{rh}$. The voltage reference v_r can then be obtained via adding $\Sigma_h v_{rh}$ to v_{r1}, which is generated by the droop controller at the fundamental frequency, e.g. the robust droop controller proposed in [34]. The resulting complete droop controller is shown in Figure 6. It is worth noting that the fundamental droop controller depends on the type of the output impedance and the fundamental droop controller adopted in Figure 6 is for inverters with resistive output impedances at the fundamental frequency. If the output impedance of the inverter at the fundamental frequency is not predominantly resistive, then the fundamental droop controller should be changed accordingly. It is worth stressing that the difficulty in defining the reactive power [26], [30] for the conventional droop controller has been avoided because the reactive power in the proposed strategy is defined at the corresponding frequency.

V. Simulation Results

Simulations were carried out with two inverters connected in parallel to verify the proposed strategy. The values of the inductors and capacitors are 2.35mH and 22μF, respectively. The fundamental frequency of the system was 50Hz and the rated output voltage was 12V RMS. The inverter load was a rectifier bridge connected to a 9Ω resistor after an LC filter with a 0.15mH inductor and a 1000μF capacitor. The inverters were designed, according to [34], to have resistive output impedances with an inner current loop shown in Figure 7. It is worth mentioning that the inner-loop controller can be designed with other methods or even removed, i.e., with $K_i = 0$. The proposed droop controller shown in Figure 6 provides the voltage reference v_r to the inner current loop shown in Figure 7. The droop controllers at the fundamental frequency were also designed according to [34] with the droop coefficients $n_1 = 2.2$ and $m_1 = 0.14$ for Inverter 1 and $n_1 = 1.1$ and $m_1 = 0.07$ for Inverter 2. The current feedback gains were chosen as $K_{i1} = 4$ and $K_{i2} = 2$ and the parameter K_e was chosen as $K_e = 20$. The 3rd and 5th harmonic droop controllers were adopted with coefficients chosen as $n_h = 5$ and $m_h = 50$.

Table I
VOLTAGE THD

Switching frequency	20 kHz	10 kHz	4 kHz
Voltage THD with the strategy	9.03%	9.4%	14.4%
Voltage THD without the strategy	16.53%	16.5%	20%

The switching frequency needs to be high enough in order to handle the 5th harmonics. Table I shows the voltage THD obtained for three different switching frequencies. It shows that the switching frequency of 4 kHz is not high enough, which resulted in a high THD. When the proposed strategy was not used, the results were also shown in Table I for comparison. The proposed strategy has considerably improved the voltage THD, by 45%. The output voltage and the inverter currents when the switching frequency was 20kHz are shown in Figure 8. The third harmonics was significantly reduced from 15% to 5% but the 5th harmonics slightly increased because of the change in the current profile caused by the reduction of the third harmonics. The two inverters shared the real power and reactive power well in the ratio of 2:1 and the voltage was maintained close to the rated voltage.

Another system consisting of two inverters rated at 230V 50Hz were simulated to show the scalability of the strategy. The parameters of the LC filters and the load were not changed (but with higher current and voltage ratings). The power consumed was around 8kVA with a power factor of 0.9. The gains of the inner loops were kept the same as well but the fundamental droop coefficients were scaled to $n_1 = \frac{2.2\times 12}{230} = 0.1148$ and $m_1 = 0.14 \times (\frac{12}{230})^2 = 3.811 \times 10^{-4}$ for Inverter 1 and $n_1 = 0.0574$ and $m_1 = 1.9055 \times 10^{-4}$ for Inverter 2 because of the change of the rated voltage and power. The harmonic droop coefficients n_h were also scaled, correspondingly, to $n_h = \frac{5\times 12}{230} = 0.2609$ and $m_h = 50 \times (\frac{12}{230})^2 = 0.1361$. The simulation was successfully run without any difficulties. The results are shown in Figure 9. Again, the THD of the voltage was significantly improved by 45%, from 17.7% to 9.77%. The third harmonics was reduced from 16% to 5% but the 5th harmonics increased slightly.

VI. EXPERIMENTAL RESULTS

Experiments were carried out with a laboratory setup, as shown in Figure 10, which consisted of two single-phase inverters controlled by dSPACE ACE1104 kits and was powered by separate 42V DC power supplies. The parameters of the inverters are the same as those in the simulations for the 12V system. The switching frequency was set at 4kHz because of the hardware limitation, partially caused by the heavy computation involved in calculating the real power and reactive power at each frequency. Due to the configuration of the hardware setup, the voltage for Inverter 2 was measured by the controller of Inverter 1 and then sent out via a DAC channel, which was then sampled by the controller of Inverter 2. This brought some latency into the system. The voltages were measured through a multiplexer, which resulted in a much lower sampling frequency for the voltage. This may have had an impact on the performance. Inverter 2 was equipped with a synchronisation mechanism, which is not described in this paper because of the page limit. Inverter 2 was synchronised with Inverter 1 when its output was not connected to that of Inverter 1 and was ready to be connected at any time.

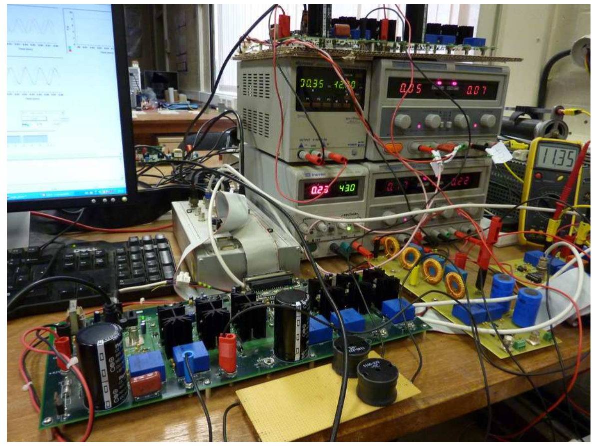

Figure 10. The experimental set-up

The experiments were carried out in three stages: 1) Inverter 1 was supplying the load; 2) Inverter 2 was put into parallel operation with Inverter 1; 3) Inverter 2 was disconnected from the parallel operation. The experimental results, after saved from dSPACE/ControlDesk and then plotted in MATLAB, are shown in the left column of Figure 11 when the proposed harmonic droop controller was not adopted and in the right column of Figure 11 when the proposed harmonic droop controller was added for the 3rd and 5th harmonics. Since the dynamic process at the fundamental frequency is much lower than that at harmonic frequencies, the dynamics of the system is dominated by that of the fundamental droop controller and the harmonic droop controller does not bring noticeable change to the response speed for the real power, the reactive power and the output voltage RMS[3]. There was no noticeable change in the steady-state performance of voltage regulation and the accuracy of power sharing, either. After the harmonic droop controller was introduced, there was significant improvement in the THD of the output voltage: from 22% to 12% for one inverter and from 15.92% to 8.57% for two inverters in parallel. This corresponds to the improvement of 46%. The 3rd harmonics was reduced from 14% to 4.5% but there was a slight increase in the 5th harmonics. The voltage THD is lower than that obtained from the simulation because of the filtering effect in the practical system.

It should be emphasised that the main purpose of this paper is to propose and demonstrate the harmonic droop controller for THD improvement, instead of reducing the THD to a certain level. Other strategies, e.g. repetitive control [2], [35],

[3]On the other hand, in order to handle high-order harmonics, the sampling speed of the controller needs to be increased.

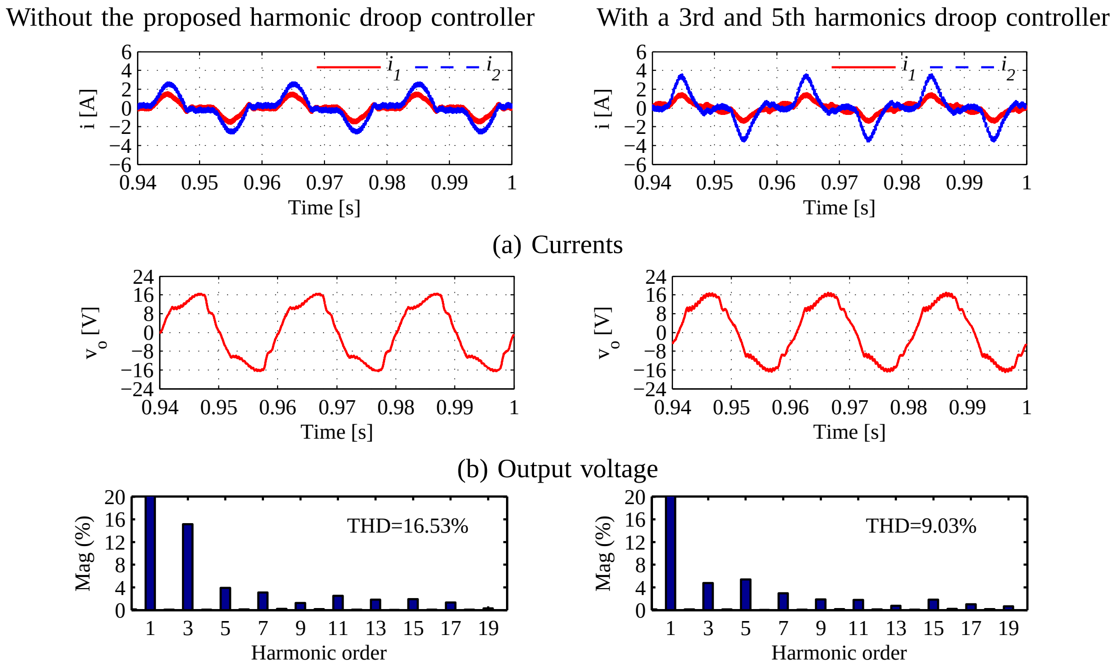

(a) Currents

(b) Output voltage

(c) Magnitude of the harmonic voltages w.r.t. the fundamental component

Figure 8. Simulation results for a 12V system: without the proposed harmonic droop controller (left column) and with a 3rd and 5th harmonics droop controller (right column).

[36] and harmonic compensation [29], can be easily combined to reduce the THD further. The LC filter of the inverter could be optimised to reduce the THD as well because the inductance L is very high for the inverters adopted in this paper. The low voltage level of the system also adds difficulties in obtaining a low THD. Indeed, a 0.12V harmonic component would have contributed to 1% THD. The switching frequency of 4kHz is not high enough to handle the 5th harmonics as shown in the previous section and also has a strong impact on the performance. After taking into account the above factors, the voltage THD of an inverter could be easily made below 5%.

VII. Conclusions

After proposing a modelling method for inverter systems, it is found out that the harmonics in an inverter system can be treated individually. A harmonic droop control strategy is then proposed to provide the right harmonic reference voltage to cancel the harmonic voltage dropped on the output impedance of the inverter, which reduces the harmonic components in the output voltage. The harmonic droop controller, which is developed after investigating the basic principles of delivering power to a constant current source (sink), does not depend on the type of the impedance. This avoids the need of checking the type for each harmonic frequency, which can be very difficult in practice. The proposed strategy also clarifies that the power sharing of inverters should be done at individual harmonic frequencies, which avoids the difficulty in defining the reactive power for different frequencies together. The proposed strategy is able to significantly reduce the harmonic components in the output voltage while accurately sharing the power at the fundamental frequency. Simulation and experimental results have shown that the proposed harmonic droop controller is able to considerably improve the THD of the output voltage. In some cases, there may still be a need to combine this strategy with others to further improve the THD.

References

[1] R. Lasseter, “Microgrids,” in *Power Engineering Society Winter Meeting, 2002. IEEE*, vol. 1, 2002, pp. 305–308 vol.1.

[2] G. Weiss, Q.-C. Zhong, T. C. Green, and J. Liang, “H^∞ repetitive control of DC-AC converters in microgrids,” *IEEE Trans. Power Electronics*, vol. 19, no. 1, pp. 219–230, 2004. [Online]. Available: http://dx.doi.org/10.1109/TPEL.2003.820561

[3] J. Guerrero, J. Vasquez, J. Matas, M. Castilla, and L. de Vicuna, “Control strategy for flexible microgrid based on parallel line-interactive UPS systems,” *IEEE Trans. Industrial Electronics*, vol. 56, no. 3, pp. 726 –736, 2009.

[4] S. V. Iyer, M. N. Belur, and M. C. Chandorkar, “A generalized computational method to determine stability of a multi-inverter microgrid,” *IEEE Trans. Power Electronics*, vol. 25, no. 9, pp. 2420 –2432, 2010.

[5] Q.-C. Zhong and G. Weiss, “Synchronverters: Inverters that mimic synchronous generators,” *IEEE Trans. Industrial Electronics*, vol. 58, no. 4, pp. 1259–1267, 2011.

[6] T. Hornik and Q.-C. Zhong, “A current control strategy for voltage-source inverters in microgrids based on H^∞ and repetitive control,” *IEEE Trans. Power Electronics*, vol. 26, no. 3, pp. 943 –952, march 2011.

[7] N. Yousefpoor, S. Fathi, N. Farokhnia, and H. A. Abyaneh, “THD minimization applied directly on the line to line voltage of multi-level inverters,” *IEEE Trans. Industrial Electronics*, no. to appear, 2011.

[8] M. Routimo, M. Salo, and H. Tuusa, “Comparison of voltage-source and current-source shunt active power filters,” *IEEE Trans. Power Electronics*, vol. 22, no. 2, pp. 636 –643, march 2007.

[9] C. Lascu, L. Asiminoaei, I. Boldea, and F. Blaabjerg, “High performance current controller for selective harmonic compensation in active power filters,” *IEEE Trans. Power Electronics*, vol. 22, no. 5, pp. 1826 –1835, sept. 2007.

[10] R. Grino, R. Cardoner, R. Costa-Castello, and E. Fossas, “Digital repetitive control of a three-phase four-wire shunt active filter,” *IEEE Trans. Industrial Electronics*, vol. 54, no. 3, pp. 1495 –1503, June 2007.

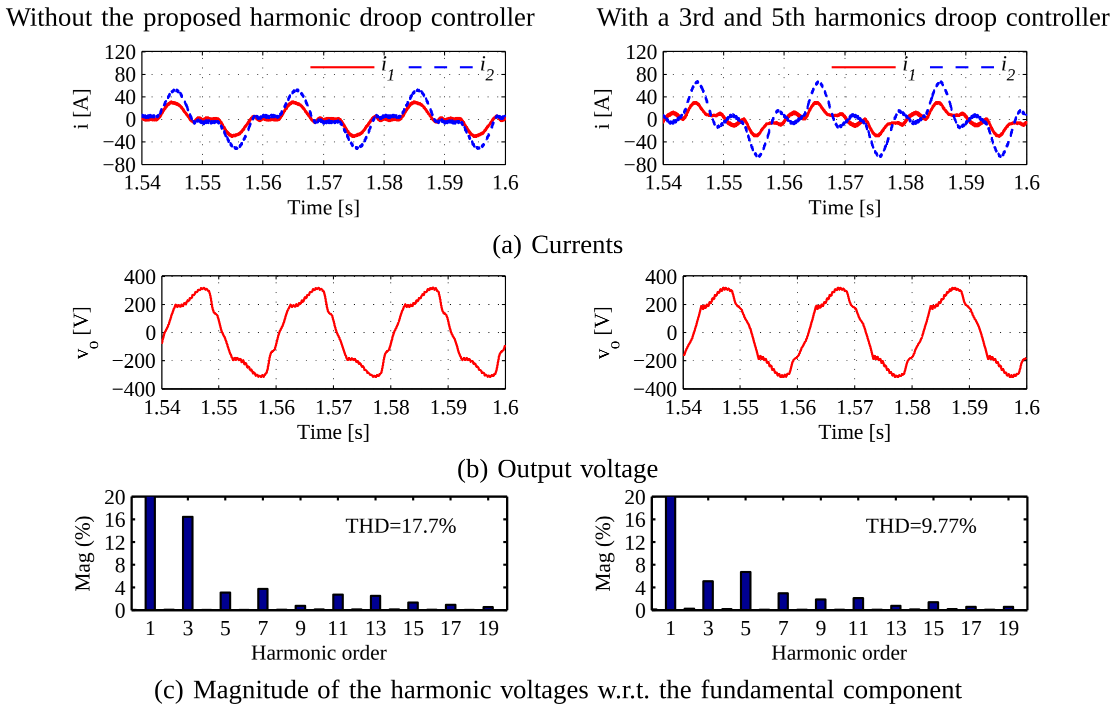

Figure 9. Simulation results for a 230V system: without the proposed harmonic droop controller (left column) and with a 3rd and 5th harmonics droop controller (right column).

[11] F. Blaabjerg, R. Teodorescu, M. Liserre, and A. V. Timbus, "Overview of control and grid synchronization for distributed power generation systems," *IEEE Trans. Industrial Electronics*, vol. 53, no. 5, pp. 1398–1409, 2006.

[12] S. Hara, Y. Yamamoto, T. Omata, and M. Nakano, "Repetitive control system: a new type servo system for periodic exogenous signals," *IEEE Trans. Automat. Control*, vol. 33, no. 7, pp. 659–668, July 1988.

[13] B. Francis and W. Wonham, "The internal model principle for linear multivariable regulators," *Applied Mathematics and Optimization*, vol. 2, pp. 170–194, December 1975.

[14] Y. Ye, B. Zhang, K. Zhou, D. Wang, and Y. Wang, "High-performance cascade-type repetitive controller for CVCF PWM inverter: analysis and design," *IET Electr. Power Appl.*, vol. 1, no. 1, January 2007.

[15] ——, "High-performance repetitive control of PWM DC-AC converters with real-time phase lead FIR filter," *IEEE Transactions on Circuits and Systems*, vol. 53, no. 8, August 2006.

[16] Y. Wang, D. Wang, B. Zhang, and K. Zhou, "Fractional delay based repetitive control with application to PWM DC/AC converters," *IEEE International Conference on Control Applications*, October 2007.

[17] B. Zhang, D. Wang, K. Zhou, and Y. Wang, "Linear phase lead compensation repetitive control of a CVCF PWM inverter," *IEEE Trans. Industrial Electronics*, vol. 55, no. 4, pp. 1595–1602, April 2008.

[18] S. Chen, Y. Lai, S.-C. Tan, and C. Tse, "Analysis and design of repetitive controller for harmonic elimination in PWM voltage source inverter systems," *IET Power Electronics*, vol. 1, no. 4, pp. 497–506, Dec. 2008.

[19] Y.-Y. Tzou, S.-L. Jung, and H.-C. Yeh, "Adaptive repetitive control of PWM inverters for very low THD AC-voltage regulation with unknown loads," *IEEE Trans. Power Electronics*, vol. 14, no. 5, pp. 973–981, September 1999.

[20] T. Hornik and Q.-C. Zhong, "H^∞ repetitive voltage control of grid-connected inverters with frequency adaptive mechanism," *IET Power Electronics*, vol. 3, no. 6, pp. 925 –935, Nov. 2010.

[21] A. Garcia-Cerrada, O. Pinzon-Ardila, V. Feliu-Batlle, P. Roncero-Sanchez, and P. Garcia-Gonzalez, "Application of a repetitive controller for a three-phase active power filter," *IEEE Trans. Power Electronics*, vol. 22, no. 1, pp. 237–246, Jan. 2007.

[22] R. Costa-Castello, R. Grino, R. Cardoner, and E. Fossas, "High performance control of a single-phase shunt active filter," *IEEE International Symposium on Industrial Electronics, ISIE*, pp. 3350–3355, June 2007.

[23] G. Weiss, Q.-C. Zhong, T. Green, and J. Liang, "H^∞ repetitive control of DC-AC converters in micro-grids," *IEEE Trans. Power Electronics*, vol. 19, no. 1, pp. 219–230, 2004.

[24] T. Hornik and Q.-C. Zhong, "H^∞ repetitive current-voltage control of inverters in microgrids," in *Proc. of the 36th Annual Conference of the IEEE Industrial Electronics Society (IECON)*, Phoenix, USA, November 2010.

[25] T.-L. Lee and P.-T. Cheng, "Design of a new cooperative harmonic filtering strategy for distributed generation interface converters in an islanding network," *IEEE Trans. Power Electronics*, vol. 22, no. 5, pp. 1919 –1927, Sept. 2007.

[26] E. Watanabe, R. Stephan, and M. Aredes, "New concepts of instantaneous active and reactive powers in electrical systems with generic loads," *IEEE Trans. Power Delivery*, vol. 8, no. 2, pp. 697 –703, apr 1993.

[27] J. Guerrero, L. Garcia de Vicuna, J. Matas, M. Castilla, and J. Miret, "Output impedance design of parallel-connected UPS inverters with wireless load-sharing control," *IEEE Trans. Industrial Electronics*, vol. 52, no. 4, pp. 1126–1135, Aug. 2005.

[28] J. Guerrero, J. Matas, L. G. de Vicuna, M. Castilla, and J. Miret, "Decentralized control for parallel operation of distributed generation inverters using resistive output impedance," *IEEE Trans. Industrial Electronics*, vol. 54, no. 2, pp. 994–1004, April 2007.

[29] Q.-C. Zhong, F. Blaabjerg, J. Guerrero, and T. Hornik, "Reduction of voltage harmonics for parallel-operated inverters equipped with a robust droop controller," in *Proc. of the 2011 IEEE Energy Conversion Congress and Exposition*, Phoenix, USA, September 2011.

[30] J. C. Montano, "Reviewing concepts of instantaneous and average compensations in polyphase systems," *IEEE Trans. Industrial Electronics*, vol. 58, no. 1, pp. 213 –220, jan. 2011.

[31] Y. Mohamed and E. El-Saadany, "Adaptive decentralized droop controller to preserve power sharing stability of paralleled inverters in distributed generation microgrids," *IEEE Trans. Power Electronics*, vol. 23, no. 6, pp. 2806 –2816, 2008.

[32] W. Yao, M. Chen, J. Matas, J. Guerrero, and Z.-M. Qian, "Design and analysis of the droop control method for parallel inverters considering the impact of the complex impedance on the power sharing," *IEEE Trans. Industrial Electronics*, vol. 58, no. 2, pp. 576 –588, 2011.

[33] J. M. Guerrero, J. C. Vasquez, J. matas, L. Garcia de Vicuna, and M. Castilla, "Hierarchical control of droop-controlled AC and DC microgrids- a general approach towards standardization," *IEEE Trans. Industrial Electronics*, vol. PP, no. 99, p. to appear, 2010.

[34] Q.-C. Zhong, "Robust droop controller for accurate proportional load sharing among inverters operated in parallel," *IEEE Trans. Industrial Electronics*, vol. 58, 2011, to appear.

[35] G. Escobar, P. Hernandez-Briones, P. Martinez, M. Hernandez-Gomez, and R. Torres-Olguin, “A repetitive-based controller for the compensation of harmonic components,” *IEEE Trans. Industrial Electronics*, vol. 55, no. 8, pp. 3150–3158, Aug. 2008.

[36] K. Zhou and D. Wang, “Digital repetitive learning controller for three-phase CVCF PWM inverter,” *IEEE Trans. Industrial Electronics*, vol. 48, no. 4, pp. 820–830, 2001.

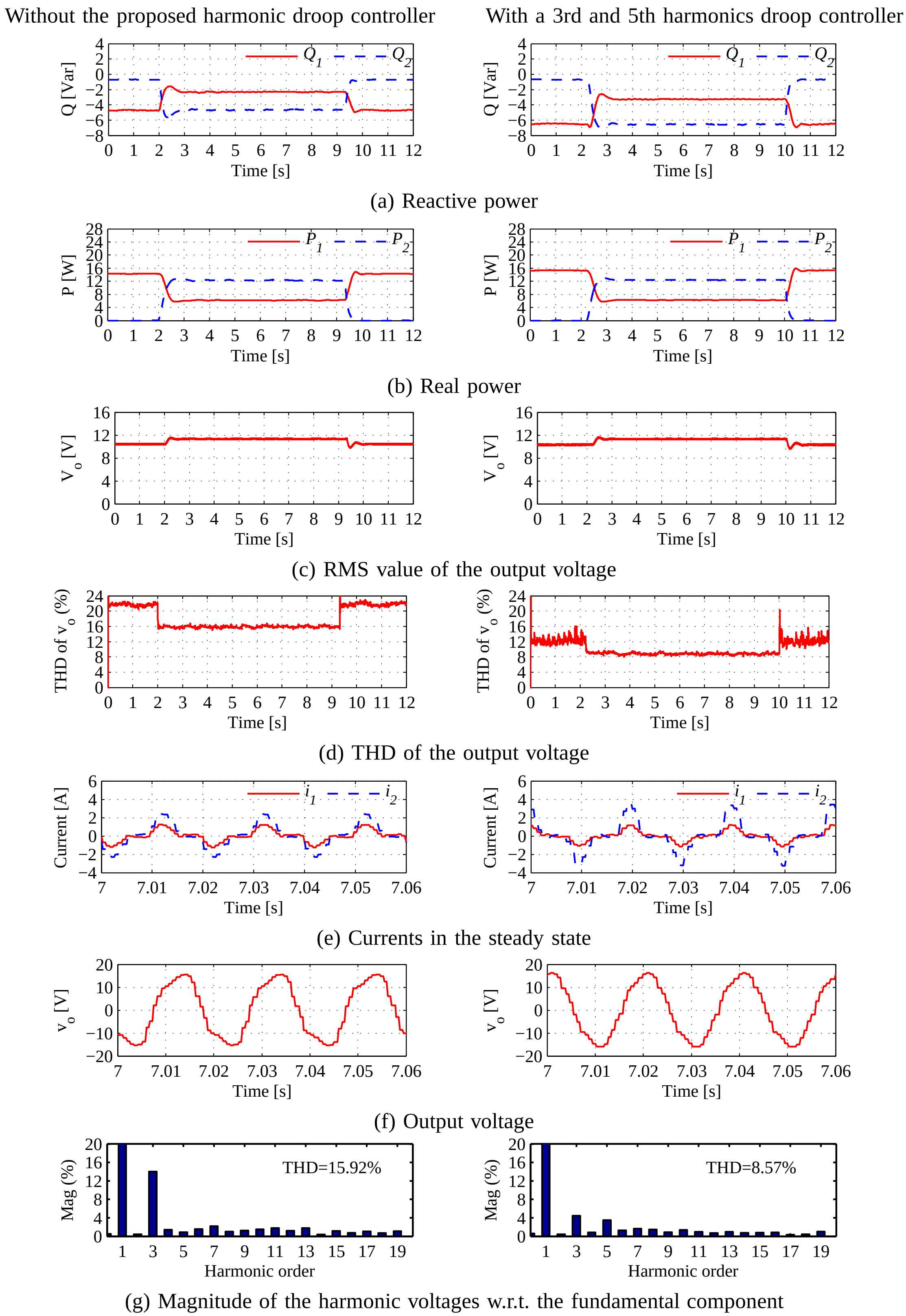

Figure 11. Experimental results: without the proposed harmonic droop controller (left column) and with a 3rd and 5th harmonics droop controller (right column).